Investigating Wireless Charging and Mobility of Electric Vehicles on Electricity Market

Chia-Ho Ou, *Member, IEEE,* Hao Liang, *Member, IEEE,* and Weihua Zhuang, *Fellow, IEEE*

Abstract—To avoid inconvenient vehicle stops at charging stations, the on-road wireless charging of electric vehicles (EVs) is a promising application in the future smart grid. In this paper, we study a critical yet open problem for this application, i.e., the impact of wireless charging and mobility of EVs on the wholesale electricity market based on locational marginal price (LMP), which is mainly determined by the EV mobility patterns. To capture the dynamics in vehicle traffic flow and state of charge (SOC) of EV batteries, we model the EV mobility as a queueing network based on the statistics obtained via traffic information systems. Then, the load on each power system bus with respect to EV wireless charging is obtained using the stationary distribution of the queueing network. An economic dispatch problem is formulated to incorporate the EV wireless charging demand, and the LMP of each power system bus is obtained. Further, a pricing mechanism based on the LMP variations of power system buses is investigated to enhance the social welfare. The performance of our proposed analytical model is verified by a realistic road traffic simulator (SUMO) based on a 3-bus test system and an IEEE 30-bus test system, respectively. Simulation results indicate that our proposed analytical model can accurately provide an estimation of the LMP variations due to EV wireless charging.

Index Terms—Electric vehicles, electricity markets, mobility, queueing networks, wireless charging.

I. INTRODUCTION

With fossil fuel depletion and increasing environmental consciousness, EVs have received significant attention due to their high fuel economy and low pollution emissions. Traditional plug-in electric vehicles (PEVs) usually recharge their batteries by plugging into the power grid (e.g., at home or on a corporate car park). With the advancement of inductive wireless power transfer (also known as contactless or plugless power transfer) technology, wireless charging becomes a promising way for EVs' charge replenishment to deal with the major drawback of the limited driving range of PEVs [1], [2]. In addition, based on the latest research results from [3], the magnetic wireless power transfer over a distance of 6.5 feet can deliver 10 kW of electric power with a coil to coil stationary efficiency of 97%. The wireless charging not only simplifies the charging process but also makes sense

C. H. Ou is with Department of Computer Science and Information Engineering, National Pingtung University, No. 51, Minsheng E. Rd., Pingtung City, Pingtung County 90004, Taiwan (e-mail: cho@mail.nptu.edu.tw).

H. Liang is with the Department of Electrical and Computer Engineering, University of Alberta, 9107-116 ST, Edmonton, Alberta, Canada T6G 2V4 (e-mail: hao2@ualberta.ca).

W. Zhuang is with the Department of Electrical and Computer Engineering, University of Waterloo, 200 University Avenue West, Waterloo, Ontario, Canada N2L 3G1 (e-mail: wzhuang@uwaterloo.ca).

economically. The charging process of EVs using wireless power transfer can be undertaken when vehicles are parked (i.e., similar to the plug-in scenario) and/or when on roads [4]. For the on-road scenario, EVs can recharge their batteries when in motion. The on-road wireless charging system can be considered as one of the unidirectional vehicle-to-grid (V2G) services [5]–[7]. Based on the V2G concept, EVs can charge their batteries and at the same time provide ancillary services (e.g., frequency regulation) for mitigating negative impacts on the power grid.

In literature, several studies have discussed impacts of EV charging on a distribution network of power systems [8]–[14]. The EV penetration has an impact on a residential distribution network because the charging of EVs may consume a large amount of energy and thus bring a high peak demand [8]–[11], power losses [12], [13], and voltage deviation [12], [14]. Several smart or optimal charging schemes are proposed to tackle the problems with EV penetration [10]–[12], [14]. However, the existing research assumes a consistent daily charging load without considering EV mobility patterns. Moreover, how to evaluate the impact of EV charging on the LMPs of a wholesale electricity market is still an open issue.

Generally, a wholesale electricity market consists of three kinds of participants, namely generation companies (GEN-COs), load-serving entities (LSEs), and an independent system operator (ISO) [15], [16]. LSEs may submit demand bids and GENCOs may provide supply offers for purchasing and selling energy at market clearing prices (i.e., LMPs) in the market. The ISO is independent from all market participants and responsible for grid operations, transmission service, and reliability. After collecting demand bids and supply offers, to maximize the social welfare, the ISO determines the LMP at each bus in the power system as well as LSE cleared demands and GENCO generation dispatch based on economic dispatch. The GENCO gets paid based on the LMP at the location of its generator. The LSE pays based on the LMP at the export location. After settlement, the LSE can resale the electricity purchased from the wholesale market to its customers at a retail price. The wholesale electricity market includes two kinds of markets: a day-ahead market and a real-time (balancing) market [17]. The day-ahead market is a forward market which develops a day-ahead hourly schedule and calculates hourly LMPs for the next operating day. On the other hand, the real-time market calculates 5-minute LMPs based on actual operating conditions of the power system for matching the instantaneous load with the instantaneous generation. The LMP or the nodal price [18] is a common method to determine energy and transmission congestion prices at specific locations. LMPs differ by location when transmission congestions occur. This is because the low cost generation cannot reach all

demands and high cost generation must be dispatched. In electricity markets, the LMP is an essential assessment for ISOs to conduct how and where to maintain market efficiency and system reliability. Therefore, the volatile LMP due to EV wireless charging is a challenging issue for power systems. The wireless charging demand can vary from location to location due to the EV mobility. As a result, the LMP can be highly sensitive to the mobility effect. In addition, the base loads (e.g., residential, commercial, or industrial loads) can be forecasted based on their historical demand profiles [19]. The EV wireless charging load cannot be accurately predicted because of the dynamics of EV mobility. A study [20] based on the plug-in charging scenario indicates that the load increase caused by recharging PEVs can significantly affect the LMP. It focuses on the daytime and nighttime charging and recharging at home or swapping battery at the battery station, under the assumption of consistent daily charging loads across zones. Yet, the mobility impact of EVs on LMP dynamics under EV wireless charging needs to be evaluated.

This paper investigates the impact of wireless charging and mobility of the EVs on the LMP. We consider a scenario where EVs can charge their batteries with the charging panels mounted on the road surfaces when EVs are in motion. First, we model the EV mobility patterns based on a queueing network to determine the spatial traffic distribution of EVs. Each EV has a psychological price (i.e., the maximum acceptable price) to make an independent charging decision. The psychological price of an EV depends on its SOC. The charging load is then analyzed based on the mobility model and SOC of the EV. Further, we formulate an economic dispatch problem to investigate the impact of wireless charging and mobility of the EVs on the LMP. From the perspective of the electricity market, a retail pricing mechanism of LSEs is presented to reduce the LMP variations. Reducing the LMP variations (i.e., the difference among the LMPs of the buses) can decrease the power generation cost such that the social welfare of electricity market can be improved. To the best of our knowledge, this work is the first study in the literature to evaluate the potential impact of EV mobility model with wireless charging on the LMP. Because the LMP can be influenced by the amount and pattern of EV wireless charging, this study can provide some insights for the LSEs to predict the EV charging loads in a realistic scenario and for the ISO to evaluate the impact of EV charging loads and to ensure the power system efficiency and reliability.

The contributions of the paper are fourfold: (1) The mobility patterns and the psychological prices of the EVs are analyzed and modeled based on a queueing network to compute EV spatial traffic distributions; (2) The EV wireless charging load is estimated based on the spatial traffic distribution and is integrated into economic dispatch; (3) An LSE pricing mechanism is introduced to adjust the retail price of wireless charging to enhance the social welfare of electricity market; (4) Realistic EV road traffic simulations are performed to evaluate the performance of the proposed queueing network model and LSE pricing mechanism.
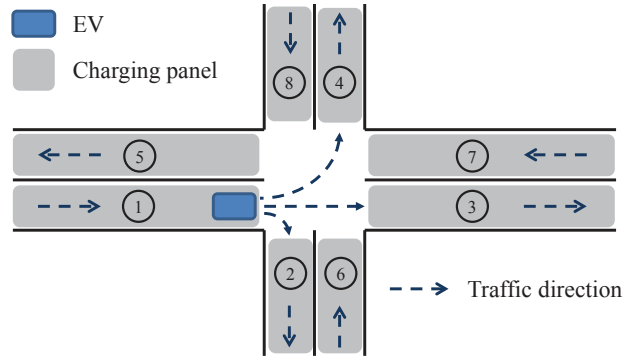

Fig. 1. A typical intersection road system and wireless charging infrastructure.

II. SYSTEM MODEL

A. EV and Road System Model

Consider a typical road system consisting of several intersections and streets. Each street corresponds to a node in the road system. Fig. 1 depicts an intersection area of a road system (with 8 nodes) and the movement directions of an EV when approaching the intersection. The wireless power transfer technology is employed in the road system. The charging panels are deployed on the surface of the streets. The EVs can withdraw energy from the power grid while moving above the charging panels.

Suppose there are M nodes in the road system and let the wireless charging power for each EV at node m ($m = 1, 2, \cdots, M$) be ξ_m. The power transfer efficiency in drawing energy from the power grid to the EV batteries is denoted by e. Each EV needs to pay for charging its battery via wireless power transfer (including power transfer loss). When an EV is moving above a charging panel, the charging decision is made by comparing its psychological price with the retail price. Consider a tagged EV with a psychological price p and a charging panel with a retail price p'. The EV charges its battery via wireless power transfer only when the retail price is not larger than its psychological price, i.e., $p' \leq p$. The psychological price of an EV depends on the SOC s of its battery which is within the range $[s_{\min}, s_{\max}]$. Without loss of generality, we consider a monotonically decreasing function $R(\cdot)$ which maps the EV SOC s ($s \in [s_{\min}, s_{\max}]$) to a psychological price p, i.e., $p = R(s)$. Intuitively, an EV with a low SOC can set a high psychological price such that its battery can be recharged more often to extend the driving range. Each EV may change its psychological price when entering a new node because of the energy usage in vehicle driving and/or the wireless charging on the road. For simplicity, we consider a homogeneous model such that all EVs in the road system have the same battery capacity ($s_{\min}$ and $s_{\max}$) and mapping function $R(\cdot)$. The average energy consumption for each EV to cover a unit distance is denoted by ζ. An extension of the model to non-homogeneous case is straightforward and will be discussed in the following section.

The statistics related to mobility patterns of EVs can be obtained by the current traffic information systems of intelligent transportation systems (ITS) [21]. Most of road traffic data

collection techniques in ITS can gather the traffic volume (e.g., hourly), trip generation rate, intersection turning movement count, and moving speed of the vehicles on a certain street.

Denote the length and average traffic speed of the street, node n ($n = 1, 2, \cdots, M$), as l_n and v_n, respectively. The average amount of energy consumed by and recharged for an EV at node n are, respectively, given by

$$E_n^c = \zeta l_n, \ E_n^r = \xi_n \tau_n = \xi_n l_n / v_n \tag{1}$$

where ζ denotes the average energy consumption for each EV to cover a unit distance (e.g., meter) and $\tau_n = l_n / v_n$ is the average sojourn time of an EV at node n. Let $r_{n,m}^*$ be the routing (or turning) probability of an EV from node n to node m. Then, we have the following traffic equation:

$$r_{n,0}^* + \sum_{m=1}^{M} r_{n,m}^* = 1, \ n = 1, 2, \cdots, M \tag{2}$$

where $r_{n,0}^*$ is the routing probability of an EV from node n to a region outside the road system. An EV may leave the network (e.g., park in the shopping mall or office building) and no longer join the traffic during a specific time. Equation (2) indicates that the sum of the routing probabilities of an EV from node n to the outside and to the inside of the road system is equal to one. Denote exogenous arrival rate as $\alpha_{m,p}^*$ which represents the rate of EVs with psychological price p arriving at node m from a region outside the road system. Note that the exogenous arrival rate may need to be estimated when EV SOC monitoring is not available in the traffic information systems and/or at the initial state of EV penetration.

B. Electricity Market Model

The wholesale electricity market model includes an ISO and a set $\mathcal{X}$ of LSEs and a set $\mathcal{Y}$ of GENCOs distributed across the buses of the power grid. The objective of the non-profit ISO is to maximize the social welfare subject to transmission constraints and GENCO generation capacity limits. With the objective, the ISO operates a day-ahead market based on the LMP mechanism. In Fig. 2, during the day before operating day, each LSE x submits a demand bid to the ISO for the operating day. The demand bid of the LSE contains two parts: base load (i.e., fixed hourly demand) to be sold at a regulated (i.e., fixed) retail price to its customers; and EV wireless charging load (i.e., price-sensitive hourly demand) to be sold at a dynamic pricing mechanism. During the day before operating day, each GENCO y reports a supply offer to the ISO for the operating day. The supply offer consists of its hourly generation cost function and the corresponding generation limit of its reported operating capacity interval. After gathering demand bids from LSEs and supply offers from GENCOs during the day before operating day, the ISO calculates and posts the hourly LMP at each bus and the dispatch generation and demand schedule to LSEs and GENCOs for the operating day. The ISO then settles the day-ahead market for the operating day by obtaining all purchase payments from LSEs and delivering all sale payments to GENCOs based on the LMPs for the operation day. It is assumed that there are no
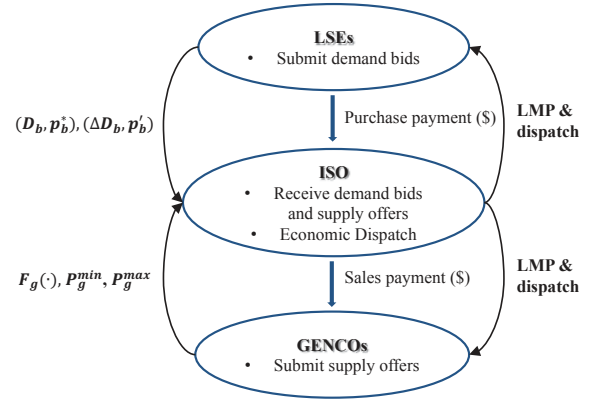

Fig. 2. The electricity market model.

disturbances or outages in the system, which means no re-bidding is required and the settlement for the day-ahead market on the day before operating day are perfectly executed as planned without additional balancing settlement in the real-time market for the difference on the operating day [16]. Without loss of generality, we focus on a specific hour of the day.

The power system in the market is composed of a set $\mathcal{B}$ of buses. Each bus b ($b \in \mathcal{B}$) has a set $\mathcal{P}_b$ of charging panels which are indexed by the corresponding nodes. For instance, if a charging panel is installed at node m and belongs to bus b, we have $m \in \mathcal{P}_b$. If LSE x owns bus b, we have $b \in \mathcal{B}_x$, where $\bigcup_{x \in \mathcal{X}} \mathcal{B}_x = \mathcal{B}$ and $\mathcal{B}_x \cap \mathcal{B}_{x'} = \emptyset$, for all $x \neq x'$, $x, x' \in \mathcal{X}$. The power system buses are connected via a set $\mathcal{L}$ of power transmission lines. If there is a transmission line connecting buses b_1 and b_2, we denote the transmission line as $(b_1, b_2) \in \mathcal{L}$. Each transmission line (b_1, b_2) is associated with a line flow limit $L_{(b_1,b_2)}^{\max}$. There is a set $\mathcal{G}$ of generators in the power system. If GENCO y owns generator g, we have $g \in \mathcal{G}_y$, where $\bigcup_{y \in \mathcal{Y}} \mathcal{G}_y = \mathcal{G}$ and $\mathcal{G}_y \cap \mathcal{G}_{y'} = \emptyset$, for all $y \neq y'$, $y, y' \in \mathcal{Y}$. A second-order cost function $F_g(\cdot)$ is typically used to represent the power generation cost of generator g [22], given by

$$F_g(P_g) = a_g P_g^2 + b_g P_g + c_g, \ g \in \mathcal{G} \tag{3}$$

where P_g is the active power output of generator g, while a_g, b_g, and c_g are the generation cost coefficients. The power output P_g of generator g is bounded by lower and upper generation limits, given by $P_g^{\min}$ and $P_g^{\max}$, respectively.

The system model focuses on the generation and transmission grids and does not involve a distribution network. That is, each LSE acts as an aggregator to combine the loads of its customers at each bus [23]. The base load (i.e., the load without EV penetration) at bus b is denoted as D_b. Let p_b^* be the fixed retail price at bus b for the base load. Moreover, we consider a uniform and dynamic retail price p_b' for EV wireless charging where all the charging panels belong to bus b. In this way, the EV charging load at bus b under the retail price p_b' is modeled as a price-sensitive demand function, i.e., ΔD_b, based on the EV mobility patterns.
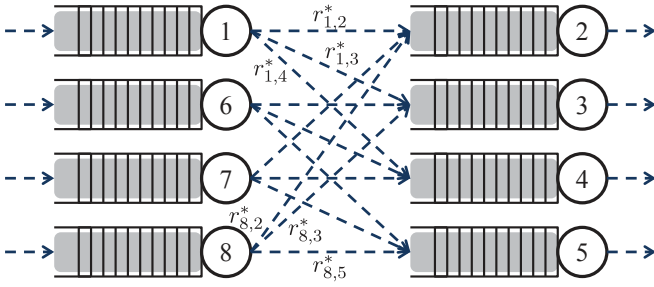
Fig. 3. The queueing network model of the typical road system.

III. ECONOMIC DISPATCH WITH EV WIRELESS CHARGING

In this section, we analyze the EV charging load for economic dispatch in electricity markets. We first analyze the EV mobility by incorporating the effect of wireless charging and then derive the charging demand function from the mobility model.

A. EV Wireless Charging Load

The EV mobility patterns are modeled as a BCMP open queueing network [24]. The streets and EVs are regarded as the nodes and customers of the queueing network, respectively. For instance, the road system in Fig. 1 can be mapped to a queueing network as shown in Fig. 3 based on the connectivity among the nodes. The traffic of node 1 can be routed to nodes 2, 3, and 4 with probabilities $r_{1,2}^*$, $r_{1,3}^*$, and $r_{1,4}^*$, respectively. Taking account of traffic equation (2), we have

$$r_{1,2}^* + r_{1,3}^* + r_{1,4}^* = 1. \tag{4}$$

Similarly, we have $r_{8,2}^* + r_{8,3}^* + r_{8,5}^* = 1$ for node 8 in Fig. 3.

For computational simplicity, we consider a finite number C of psychological price categories. The categories of psychological prices of an EV can be, for example: very low, low, medium, high, and very high. The price category c ($c = 1, 2, \cdots, C-1$) corresponds to a SOC within the range $[s_{c-1}, s_c)$, where $s_0 = s_{\min}$ and $s_{c-1} < s_c$ for all $c = 1, 2, \cdots, C-1$. For the price category C, the corresponding SOC range is $[s_{C-1}, s_C]$, where $s_C = s_{\max}$ and $s_{C-1} < s_C$. Based on the SOC-price mapping function $R(\cdot)$, the equivalent psychological price of category c can be calculated by

$$p_c = \frac{R(s_c) + R(s_{c-1})}{2}. \tag{5}$$

Accordingly, we aggregate the exogenous arrival rate for each psychological price category. The aggregated exogenous arrival rate of EVs with psychological price category c at node m is given by

$$\alpha'_{m,c} = \sum_{p \in [R(s_{c-1}), R(s_c)]} \alpha_{m,p}^*. \tag{6}$$

It is worth mentioning that the above categorization (or quantization) can facilitate our queueing network analysis since the EVs with different psychological prices are categorized into a finite (and potentially smaller) number of classes. A more accurate mobility model can be obtained by choosing a larger C at the cost of a higher computational complexity, and

vice versa. Moreover, in order to extend the mobility model to a non-homogeneous case such that different EVs have different energy storage and consumption characteristics, more classes (C) can be defined by incorporating the manufacturer and/or models of EVs. The proposed analytical model can be directly applied by increasing the number of classes.

The load of EV wireless charging is measured by the spatial EV traffic distribution within the charging areas. Based on the mobility model, we consider each node at the queueing network as an M/G/∞ node with C customer classes corresponding to the EV's psychological price categories. With the BCMP network, the arrival rate ($\alpha_{m,c}$) of class-c ($c = 1, 2, \cdots, C$) customers at node m ($m = 1, 2, \cdots, M$) in the queueing network satisfies the following equation:

$$\alpha_{m,c} = \alpha'_{m,c} + \sum_{n=1}^{M} \sum_{k=1}^{C} \alpha_{n,k} r_{nk,mc} \tag{7}$$

where $r_{nk,mc}$ is the routing probability of a customer from class-k at node n to class-c at node m. Suppose node n belongs to bus b, i.e., $n \in \mathcal{P}_b$. Taking account of the routing probability without psychological price ($r_{n,m}^*$) and energy consuming/recharging process, the value of $r_{nk,mc}$ can be calculated. If $k \neq c$, we have

$$r_{nk,mc} = \begin{cases} r_{n,m}^* \cdot \frac{E_n^r - E_n^c}{s_k - s_{k-1}}, & \text{if } c = k-1 \text{ and } p_k \geq p_b' \\ & \text{and } E_n^r > E_n^c \\ r_{n,m}^* \cdot \frac{E_n^c - E_n^r}{s_k - s_{k-1}}, & \text{if } c = k+1 \text{ and } p_k \geq p_b' \\ & \text{and } E_n^c > E_n^r \\ r_{n,m}^* \cdot \frac{E_n^c}{s_k - s_{k-1}}, & \text{if } c = k+1 \text{ and } p_k < p_b' \end{cases} \tag{8}$$

where the first case corresponds to the recharging of a class-k EV at node n. If the recharged energy (E_n^r) is larger than the consumed energy (E_n^c), the probability for the EV to decrease its psychological price by one level can be approximated as $\frac{E_n^r - E_n^c}{s_k - s_{k-1}}$. Similarly, the second case in (8) corresponds to the recharging of a class-k EV at node n, given the recharged energy is less than the consumed energy. The third case in (8) denotes the routing probability without EV recharging. For all other cases with $k \neq c$ and not mentioned in (8), we have $r_{nk,mc} = 0$. If $k = c$, the value of $r_{nk,mc}$ can be calculated based on a complementary of (8) with respect to the routing probability without psychological price ($r_{n,m}^*$), given by

$$r_{nk,mc} = r_{n,m}^* - \sum_{i=1}^{C} \sum_{\substack{j=1 \\ j \neq i}}^{C} r_{ni,mj}. \tag{9}$$

Using queueing network analysis, we can obtain the stationary distribution for different numbers of EVs of different price categories in different streets as follows:

$$\pi(\mathbf{n}) = \prod_{m=1}^{M} \pi_m(\mathbf{n}_m) \tag{10}$$

where $\mathbf{n} = (\mathbf{n}_1, \cdots, \mathbf{n}_M)$, $\mathbf{n}_m = (n_{m,1}, \cdots, n_{m,C})$, and $n_{m,c}$ ($n_{m,c} = 0, 1, 2, \cdots, n_{\max}$) is the number of class-c customers at node m. Here, $n_{\max}$ is the maximum possible number of
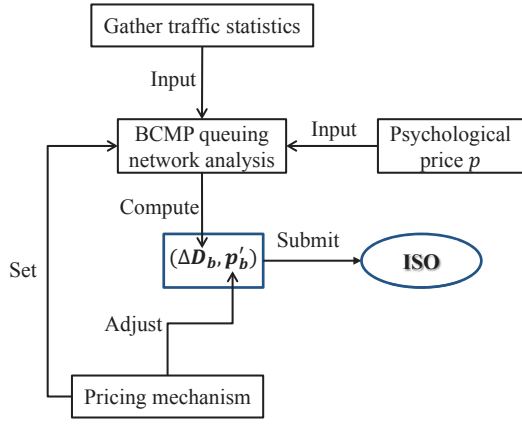
Fig. 4. The proposed analytical model and pricing mechanism.

EVs of one class at a specific node. Further, we have

$$\pi_m(\mathbf{n}_m) = e^{-\rho_m} \prod_{c=1}^{C} \frac{\rho_{m,c}^{n_{m,c}}}{n_{m,c}!} \tag{11}$$

where $\rho_m = \sum_{c=1}^{C} \rho_{m,c}$, $\rho_{m,c} = \frac{\alpha_{m,c}}{\mu_m}$, and μ_m is the average service rate of customers at node m which is the reciprocal of the average sojourn time, i.e., $\mu_m = \frac{1}{\tau_m}$.

Given the stationary distribution, the load increment caused by EV wireless charging at bus b (i.e., the price-sensitive demand function) can be calculated as

$$\Delta D_b = \sum_{m \in \mathcal{P}_b} \frac{\xi_m}{e} \left[\sum_{\mathbf{n}_m} (\sum_{c=1}^{C} n_{m,c} I(p_c \geq p_b')) \pi_m(\mathbf{n}_m) \right] \tag{12}$$

where $\frac{\xi_m}{e}$ represents the wireless power transfer for each EV at node m taking account of power transfer efficiency, $\sum_{\mathbf{n}_m} = \sum_{n_{m,1}=0}^{n_{max}} \sum_{n_{m,2}=0}^{n_{max}} \cdots \sum_{n_{m,C}=0}^{n_{max}}$ represents a summation over all possible values of $\mathbf{n}_m$, and $I(A)$ is an indication function which equals 1 if event A is true and 0 otherwise. In (12), only the EVs with psychological prices not less than the retail price (i.e., $p_c \geq p_b'$) can recharge their batteries and, thus, are included in the EV wireless charging load calculation. As shown in Fig. 4, the price-sensitive demand function ΔD_b with the retail price p_b' is fed by the traffic statistics and the psychological price p of the EVs. After computation, the wireless charging demand is included in the demand bid and then submitted to the ISO.

B. Economic Dispatch

A direct current (DC) lossless load flow model is used to formulate the economic dispatch problem with the objective of social welfare maximization such that the impact of wireless charging and mobility of EVs on LMPs can be investigated. Consider a specific hour of the operating day. The social

welfare (SW) function is derived in [15], given by

$$
\begin{aligned}
SW &= \sum_{x \in \mathcal{X}} R_x - \sum_{y \in \mathcal{Y}} C_y \\
&= \sum_{x \in \mathcal{X}} \sum_{b \in \mathcal{B}_x} (p_b^* \cdot D_b + p_b' \cdot \Delta D_b) - \sum_{y \in \mathcal{Y}} \sum_{g \in \mathcal{G}_y} F_g(P_g) \\
&= \sum_{b \in \mathcal{B}} (p_b^* \cdot D_b + p_b' \cdot \Delta D_b) - \sum_{g \in \mathcal{G}} F_g(P_g) \tag{13}
\end{aligned}
$$

where R_x denotes the revenues of LSE x from the resale of power to its retail customers of the base load and the wireless charging, and C_y denotes the generation cost for GENCO y.

To maximize the social welfare, the economic dispatch problem is given by

$$(\mathbf{P1}) \max_{P_g (g \in \mathcal{G})} \quad SW \tag{14}$$

$$\text{subject to} \quad \sum_{g \in \mathcal{G}} P_g = \sum_{b \in \mathcal{B}} (D_b + \Delta D_b) \tag{15}$$

$$P_g^{\min} \leq P_g \leq P_g^{\max}, \ g \in \mathcal{G} \tag{16}$$

$$-L_{(k,m)}^{\max} \leq L_{(k,m)} \leq L_{(k,m)}^{\max}, \ (k,m) \in \mathcal{L} \tag{17}$$

where $L_{(k,m)}$ denotes the active power flow from bus k to bus m, given by

$$L_{(k,m)} = \sum_{b \in \mathcal{B}} A_{(k,m)}^{b} (PG_b - PD_b) \tag{18}$$

with $A_{(k,m)}^{s}$ representing the sensitivity coefficient which depends on the impedances of power transmission lines [22]. The objective of the economic dispatch problem is to maximize the social welfare which is the difference between the revenue of the LSEs and the power generation cost of the GENCOs as shown in (14). Constraint (15) states that the total power generation should be equal to the total demand including wireless charging load. Constraint (16) is the generator limits constraint. Constraint (17) indicates that the transmission capacity limit is applied to each power transmission line in both directions.

The economic dispatch problem belongs to a class of convex optimization problem since the objective function is concave (with respect to maximization) while all constraints are linear [25]. Therefore, it can be efficiently solved by an interior point method [22]. By solving the optimization problem, the LMP variation due to wireless charging and mobility of EVs can be measured. The LMP of each bus in the system is determined by the optimal solution of the economic dispatch problem and the associated Lagrangian multiplier of the solution [18].

C. LSE Pricing Mechanism

Suppose the retail price of the LSEs for the base load (p_b^*) is a constant. An LSE pricing mechanism which adjusts the retail price for EV wireless charging (p_b'), is presented to reduce the LMP variations and further maximize the social welfare of the electricity market (see Fig. 4). Generally, the psychological prices of the EV owners can be obtained based

on a market survey. Without loss of generality, assume that $p'_b \in [p_1, p_C]$ where p_1 and p_C denote the minimum and the maximum psychological price of the EV owners, respectively, as mentioned in Section II. An EV does not charge its battery when the retail price is higher than its psychological price. The EV may choose the other locations for charging while traveling on the road. As the retail price p'_b increases, the wireless charging load and thus the LMP of bus b decrease. However, the social welfare may reduce if the wireless charging load is reduced extensively, which results in much less electricity transactions.

The economic dispatch problem with the proposed pricing mechanism can be formulated as

$$(\textbf{P2}) \quad \max_{p'_b \in [p_1, p_C], P_g(g \in \mathcal{G})} SW \quad (19)$$

$$\text{subject to} \quad (15), (16), (17).$$

Then, the following proposition holds.

Proposition 1: Given retail price $p_j + \delta$ at bus b, where $b \in \mathcal{B}$, $j = 1, 2, \cdots, C - 1$, and $\delta \in (0, p_{j+1} - p_j]$. The load increment caused by EV wireless charging at bus b under the retail price $p_j + \delta$ is equal to that under the retail price p_{j+1}, i.e., $\Delta D_b^{p_j+\delta} = \Delta D_b^{p_{j+1}}$, where $\Delta D_b^{p_j+\delta}$ and $\Delta D_b^{p_{j+1}}$ are calculated based on (12) by replacing p'_b with $p_j + \delta$ and p_{j+1}, respectively.

Proof: As presented in Subsection III-A, the stationary distribution for different numbers of EVs of different price categories in different streets is required for computing the loads of EV wireless charging. In the proposed analytical model, the routing probability of a customer from class-k at node n ($n \in \mathcal{P}_b$) to class-c at node m ($r_{nk,mc}$) is dependent on the retail price p'_b as shown in (8).

First, we need to prove that $r_{nk,mc}$ under the retail price $p_j + \delta$ is equal to that under the retail price p_{j+1}. For the retail price $p_j + \delta$ and $k \neq c$, we have

$$r_{nk,mc}^{p_j+\delta} = \begin{cases} r_{n,m}^* \cdot \frac{E_n^r - E_n^c}{s_k - s_{k-1}}, & \text{if } c = k - 1 \text{ and } p_k \geq p_j + \delta \\ & \text{and } E_n^r > E_n^c \\ r_{n,m}^* \cdot \frac{E_n^c - E_n^r}{s_k - s_{k-1}}, & \text{if } c = k + 1 \text{ and } p_k \geq p_j + \delta \\ & \text{and } E_n^c > E_n^r \\ r_{n,m}^* \cdot \frac{E_n^c}{s_k - s_{k-1}}, & \text{if } c = k + 1 \text{ and } p_k < p_j + \delta. \end{cases} \quad (20)$$

For the retail price p_{j+1} and $k \neq c$, let

$$r_{nk,mc}^{p_{j+1}} = \begin{cases} r_{n,m}^* \cdot \frac{E_n^r - E_n^c}{s_k - s_{k-1}}, & \text{if } c = k - 1 \text{ and } p_k \geq p_{j+1} \\ & \text{and } E_n^r > E_n^c \\ r_{n,m}^* \cdot \frac{E_n^c - E_n^r}{s_k - s_{k-1}}, & \text{if } c = k + 1 \text{ and } p_k \geq p_{j+1} \\ & \text{and } E_n^c > E_n^r \\ r_{n,m}^* \cdot \frac{E_n^c}{s_k - s_{k-1}}, & \text{if } c = k + 1 \text{ and } p_k < p_{j+1}. \end{cases} \quad (21)$$

It can be observed that, when $k \geq j+1$, conditions $p_k \geq p_j + \delta$ and $p_k \geq p_{j+1}$ are satisfied in (20) and (21), respectively. On the other hand, when $k < j + 1$, conditions $p_k < p_j + \delta$ and $p_k < p_{j+1}$ are satisfied in (20) and (21), respectively. Hence, the routing probability of a customer from class-k at node n to class-c at node m under the market price $p_j + \delta$ is equal to that under the market price p_{j+1}, i.e., $r_{nk,mc}^{p_j+\delta} = r_{nk,mc}^{p_{j+1}}$.

Therefore, the stationary distribution for different numbers of EVs of different price categories in different streets of the proposed model under two different prices ($p_j + \delta$ and p_{j+1}) is identical.

In the following, we prove that the load increments caused by EV wireless charging calculated based on the given stationary distribution under the two retail prices are equal. In (12), $I(p_i \geq p'_b)$ is an indication function to determine the charging decisions made by the EV owners and is sensitive to the retail price in our LSE pricing mechanism. Two cases, $i \geq j + 1$ and $i < j + 1$ where $i, j = 1, 2, \cdots, C - 1$ are considered in the following discussion. In the first case ($i \geq j + 1$), since $\delta \in (0, p_{j+1} - p_j]$, the relation between the indication functions given the two market prices is given by

$$I(p_i \geq p_j + \delta) = I(p_i \geq p_{j+1}) = 1. \quad (22)$$

In the second case ($i < j + 1$), we have

$$I(p_i \geq p_j + \delta) = I(p_i \geq p_{j+1}) = 0. \quad (23)$$

In other words, the load increment caused by EV wireless charging at bus b under the market price $p_j + \delta$ is equal to that under the market price p_{j+1}, i.e.,

$$\begin{aligned} \Delta D_b^{p_j+\delta} &= \sum_{m \in \mathcal{P}_b} \xi_m \left[\sum_{\mathbf{n}_m} (\sum_{c=1}^{C} n_{m,c} I(p_c \geq p'_b)) \pi_m(\mathbf{n}_m) \right] \\ &= \sum_{m \in \mathcal{P}_b} \xi_m \left[\sum_{\mathbf{n}_m} (\sum_{c=1}^{C} n_{m,c} I(p_c \geq p_{j+1})) \pi_m(\mathbf{n}_m) \right] \\ &= \Delta D_b^{p_{j+1}}. \end{aligned} \quad (24)$$

∎

According to proposition 1 and $p_{j+1} \geq p_j + \delta$, we have the following inequality for the objective function of problem P2:

$$\begin{aligned} & \sum_{b \in \mathcal{B}} (p_b^* \cdot D_b + p_{j+1} \cdot \Delta D_b^{p_{j+1}}) - \sum_{g \in \mathcal{G}} F_g(P_g) \\ &= \sum_{b \in \mathcal{B}} (p_b^* \cdot D_b + p_{j+1} \cdot \Delta D_b^{p_j+\delta}) - \sum_{g \in \mathcal{G}} F_g(P_g) \\ &\geq \sum_{b \in \mathcal{B}} (p_b^* \cdot D_b + (p_j + \delta) \cdot \Delta D_b^{p_j+\delta}) - \sum_{g \in \mathcal{G}} F_g(P_g). \quad (25) \end{aligned}$$

Based on the inequality (25), the LSE making the retail price as an integer p_{j+1} instead of the values of $p_j + \delta$ can achieve a higher social welfare, while the constraints in problem P2 are still feasible. Problem P2 is thus transformed into the following problem:

$$(\textbf{P3}) \quad \max_{p'_b \in \{p_j | j = 2, 3, \cdots, C\}, P_g(g \in \mathcal{G})} SW \quad (26)$$

$$\text{subject to} \quad (15), (16), (17).$$

Problem P3 is a mixed integer non-linear programming (MINLP) problem, which is NP-hard [26]. In general, there is no efficient method to solve the problem. However, when the scale of the road system is small, an exhaust search method can be used to solve the problem. More efficient methods to solve the MINLP problem need further investigation.

D. Discussion on the Scale of Road System

Our proposed analytical model can provide an efficient method for LSE pricing mechanism without requiring time-consuming real world experiments. However, when mapping the power system infrastructure (i.e., power system buses and transmission lines) to the road map, a large-scale road system (which includes a huge number of charging panels per system bus) may be used in the proposed analytical model. To reduce the computational complexity, we can divide the large-scale road system into several small-scale road regions. The inter-region traffic flow is reflected by the exogenous arrival rate ($\alpha^*_{m,p}$) and routing probability to an adjacent region ($r^*_{n,0}$). After calculating the charging demand of each region, the total load due to EV wireless charging can be obtained.

IV. Case Study - 3-Bus Test System

To study the impact of EV wireless charging on LMPs, we consider a 3-bus test system similar to the ones used in [22], [23]. Simulations of realistic EV mobility are performed based on the road traffic simulator (SUMO) [27]. SUMO is an open-source traffic simulator and is capable of accurately modeling the behavior of individual drivers by considering vehicle-to-vehicle and vehicle-to-road signalization interactions and has been validated by the transportation research community. The battery and energy consumption statistics of an off-the-shelf plug-in hybrid electric vehicle Chevrolet Volt [28] are used in the case study. The proposed BCMP network model is implemented in Matlab, and the economic dispatch problem is implemented using a well-known Matlab-based power system simulation package, MATPOWER [29]. Specifically, MAT-POWER is an open-source simulation package and can be customized by adding user-defined variables, costs, and constraints. In this case study, a MATPOWER M-file [29] which specifies the system configuration of a 3-bus test system [30] is created for performance evaluation. The traffic statistics of the BCMP network model are fed using the SUMO simulation results according to Fig. 4.

A. System Topology and Configuration

A 3-bus test system is considered in the case study. Three LSEs and three GENCOs involve in the electricity market. Each bus has one LSE and one GENCO for load serving and power supply respectively [16]. The topology of the 3-bus test system is shown in Fig. 5. The parameters of the generators, base loads, and transmission lines are given in [30]. In our simulations, the topology of the 3-bus test system is mapped to a typical Manhattan-style road system in a high traffic and populated area (see Fig. 5). The road system is a 4×4 km^2 region and is composed of 9 intersections and 24 streets (two-way). Each street has a length of 2 km with two lanes and the vehicular movements in the intersections are controlled by traffic signals. The charging panels of red region (8 streets), green region (6 streets), and blue region (10 streets) belong to bus 1, bus 2, and bus 3, respectively. This setting implies that region 3 has the highest potential traffic volume and thus the highest EV wireless charging load.
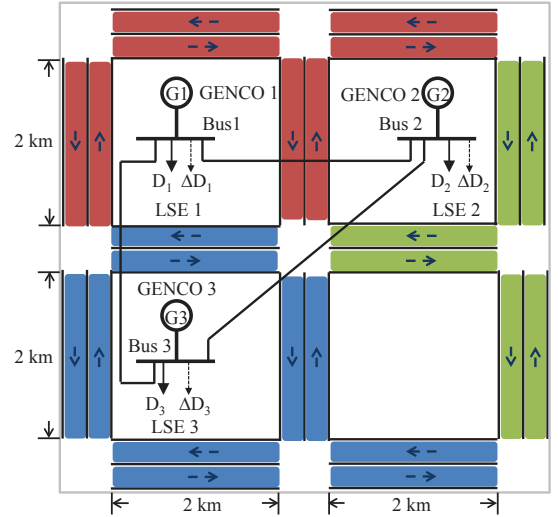
Fig. 5. The topology of 3-bus test system with mapped road system.

B. Traffic Generation

We assume that the EVs arrive at the road system from each street according to a Poisson process. The exogenous arrival rate at each street is selected such that the average traffic volume is consistent with real road systems. Specifically, we consider the average annual daily traffic (AADT) of the roads to be between 50,000 and 100,000 based on Washington State 2011 peak hour report [31]. The result shows that the average hourly traffic volume is about $71,540/24 = 2980.83$ vehicle per street. Different exogenous arrival rates are evaluated to match the average hourly traffic volume. According to SUMO simulation results, an exogenous arrival rate 0.2 vehicle/s can generate an average traffic volume 3,360 in the proposed road map and is used in the following case study. Each EV randomly selects a street in the road system as its destination. According to the Electric Power Research Institute, the EV penetration level can reach 35%, 51%, and 62% by 2020, 2030, and 2050, respectively [32]. Therefore, we considered a series of market penetration levels of EVs from 10% to 60% of the total traffic volume.

C. Battery Model and Wireless Charging

The battery model is based on the parameters reported by Chevrolet Volt which uses a lithium-ion battery (Li-ion) battery pack [28]. The battery pack provides 16 kWh energy storage capacity, while a vehicle only uses about 10 kWh of this capacity to extend the battery's lifetime based on an energy management system. The energy consumption for driving is 0.2 kWh/km. The initial EV SOC is randomly selected between 1 kWh and 9 kWh (or equivalently, 10% and 90% of the available capacity). The wireless charging power for each charging panel is 10 kW [3]. According to [4], the *average* power transfer efficiency from the power grid to the EVs battery under varying mobility conditions is 80%. To obtain a positive social welfare, the retail price of the LSEs for the base load is set at 4 cent/kWh based on the generation cost of the GENCOs, as shown in (13). In general, the retail price
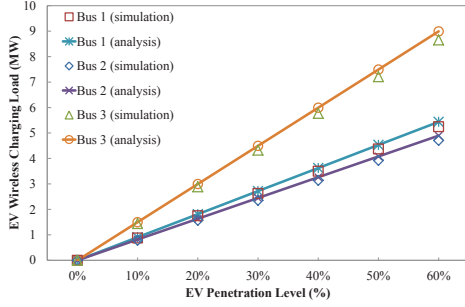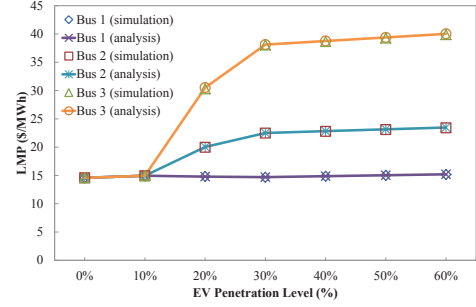
Fig. 6. EV wireless charging load versus EV penetration level.

Fig. 7. LMP versus EV penetration level.

Fig. 8. Social welfare versus EV penetration level.

for wireless charging should be more expensive than that for the base load. Thus, the retail prices for wireless charging (i.e., from 4.5 to 6.5 cent/kWh) are set exceeding the retail price for the base load (i.e., 4 cent/kWh). The psychological price of an EV consists of 5 levels (i.e., 4.5, 5, 5.5, 6, and 6.5 cent/kWh) corresponding to the 5 levels of SOC (i.e., [8,10], [6,8], [4,6], [2,4], and [0,2) kWh).

The retail price for wireless charging of a road is available for the EV owners based on ITS. When an EV owner is driving on a road, he/she compares his/her psychological price with the retail price of the road. If the retail price is higher than the psychological price, the EV owner does not charge his/her battery. With the price information, the EV owner charges his/her battery when moving on road segments with less expensive prices (from his/her own point of view). Each EV owner thus can be satisfied with charging service from LSEs.

D. Impact of EV Penetration Level

Fig. 6 illustrates the variation of the EV wireless charging load with the EV penetration level in the simulated road system. The retail price of the LSEs for wireless charging is 4.5 cent/kWh. It is observed that in both analytical and simulation results, the wireless charging loads of all buses increase gradually as the penetration level increases from 10% to 60%. As expected, the load on the bus 3 is more than those of the other two buses. This is because bus 3 contains more charging panels, as described in Subsection IV-A. The charging loads calculated based on the proposed BCMP network model are very close to those based on simulations. In other words, the proposed BCMP network model can accurately estimate the load due to EV wireless charging given the EV mobility statistics collected from traffic information systems.

Fig. 7 shows that the LMP variations for both BCMP network analysis and simulation increase as the penetration level increases from 10% to 60%. The analytical result of the proposed model matches well with that of realistic simulation using SUMO simulator. Obviously, the LMPs of three buses remain at a uniform LMP as the penetration level is lower than 20%. However, when the penetration level achieves 20%, an LMP separation appears because line $(1,3)$ is congested (see Fig. 5). Compared with the LMPs without EV wireless charging, the LMPs of bus 1, bus 2, and bus 3 are raised by 4%, 60%, and 173%, respectively. It is evident that the LMP
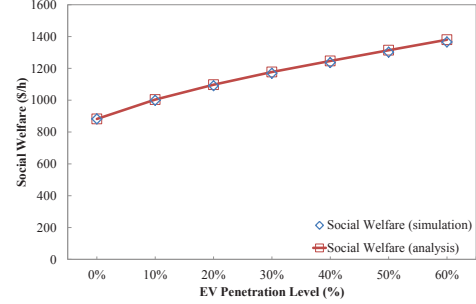
of a bus can be increased due to the EV wireless charging demand. In other words, the power generator with the higher generation cost needs to be dispatched to serve the EV wireless charging demand.

As shown in Fig. 8, the social welfare of electricity market obtained from the analysis and the simulation increase from $882.35 per hour to $1,365.65 per hour and $1,379.99 per hour, respectively, as the penetration level increases from 10% to 60%. With a higher wireless charging demand, the increase of the revenue of the LSEs is still higher than the power generation cost of the GENCOs, as shown in (13). To improve the social welfare, LSEs may raise retail prices for wireless charging. However, the social welfare may decrease accordingly because the demand of EV wireless charging is suppressed by high retail prices, to be discussed in the following subsection.

E. Impact of LSE Pricing Mechanism

The LSE pricing mechanism enables the LSEs to change their retail prices for wireless charging to enhance the social welfare. In this subsection, we assume that all the LSEs set the same retail price on each bus. In the following evaluation, the EV penetration level is set to be 60% of the total traffic volume. Fig. 9 compares the wireless charging load on each bus under different pricing schemes (i.e., 4.5, 5, 5.5, 6, and 6.5 cent/kWh). The analytical results based on the proposed BCMP network model are also close to the simulation results. The proposed model successfully predicts the charging load of different pricing mechanisms. It is observed that the wireless charging loads dramatically decrease as the retail price for wireless charging raises. The main reason is that wireless
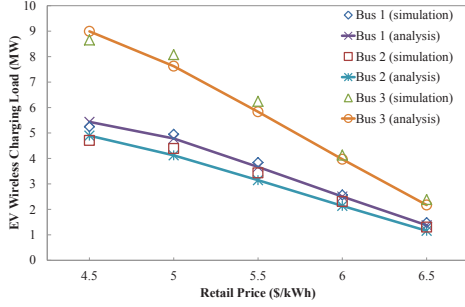
Fig. 9. EV wireless charging load versus pricing mechanism.

Fig. 11. Social welfare versus pricing mechanism.
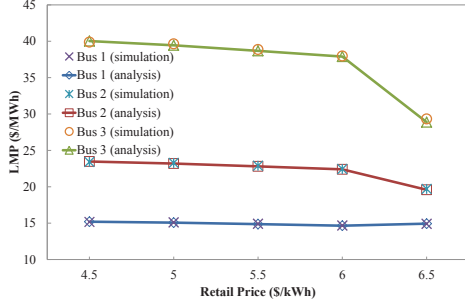
Fig. 10. LMP versus pricing mechanism.

charging on the road is not carried out for most EVs as the retail price is higher than their psychological prices, and thus the wireless charging demand is restrained by higher retail prices.

Fig. 10 depicts the LMP variations on each bus under different pricing mechanisms. It is obvious that raising the LSE retail price indeed suppresses the growth of LMPs. Both analytical and simulation results indicate that the LMPs of bus 1 and bus 2 can be reduced to the values closer to those with only the base load. The LMP variation of bus 3 is reduced from 173% to 28% as the retail price is increased to 6.5 cent/kWh. However, the LMP separation remains because the congestion of line $(1, 3)$ is not released.

Fig. 11 illustrates the social welfare for various pricing mechanisms in the price range from 4.5 to 6.5 cent/kWh. It is observed that the social welfare calculated from both analysis and simulation do not always increase with the retail price. As shown in Fig. 11, a retail price of 5 cent/kWh achieves the highest social welfare. If a higher retail price is chosen by the LSE, the wireless charging demand decreases accordingly (see Fig. 9). In other words, the reduction in the revenues of the LSEs may surpass the reduction in power generation cost of the GENCOs as the number of EV charging on the road decreases. In the following, we vary the retail price for each LSE to investigate impact of the pricing mechanism on different buses.

Among all combinations of the retail price from 4.5 to 6.5 cent/kWh for the three buses, the maximum social welfare is achieved in both the analytical and simulation results when the retail price of bus 3 is set to 5.5 cent/kWh and the retail price of other two buses is set to 5 cent/kWh. If the retail price of bus 3 increases, the wireless charging load on
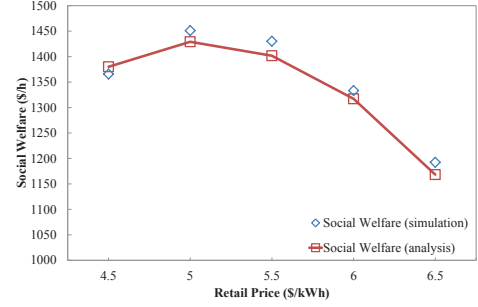
the bus decreases accordingly. This result implies that power generation cost can be further reduced because the LMP of bus 3 is much higher than those of the other two buses (see Fig. 10). That is, the social welfare can be improved by increasing the retail price of the bus with a higher LMP.

V. CASE STUDY - IEEE 30-BUS TEST SYSTEM

In this section, we present the performance evaluation of the proposed analytical model on an IEEE 30-bus test system. Based on the similar system and traffic configurations and EV battery and wireless charging model in Section IV, the IEEE 30-bus test system similar to the one used in [33] is considered for studying the impact of EV wireless charging on the LMP. The system configuration of the IEEE 30-bus test system [35] is specified in an M-file in MATPOWER for executing simulations.

A. System Topology and Configuration

In the IEEE 30-bus test system, 30 LSEs and 9 GENCOs participate in the electricity market. Each LSE provides load serving on a bus and each GENCO owns a power generator on a bus for power supply [16]. The topology of the IEEE 30-bus test system [34] is shown in Fig. 12, where the IDs of the generators are in accordance with [33] and are marked beside the corresponding buses. The parameters of the generators, base loads, and transmission lines are given in [35]. The topology of the 30-bus test system is also mapped to a 20×20 km^2 Manhattan-style road system composed of 121 intersections and 440 streets. Each street has two lanes and its length is 2 km. For simplicity, we divide the topology with the road system into three areas, i.e., area 1 (199 streets, 16 buses), area 2 (128 streets, 7 buses), and area 3 (113 streets, 7 buses), as shown in Fig. 12. The charging panels of the buses within each area have a uniform retail price. Based on SUMO simulation results, an exogenous arrival rate 0.11 vehicle/s can generate an average hourly traffic volume 3,354 in the road system and is selected in the case study. The destination (i.e., a street) of each EV is randomly chosen from the road system. We consider 60% of the total traffic volume as the market penetration level of EVs.

B. Results

Without the EV penetration, the average LMP among the buses is 22.87 dollar/MWh and the social welfare is
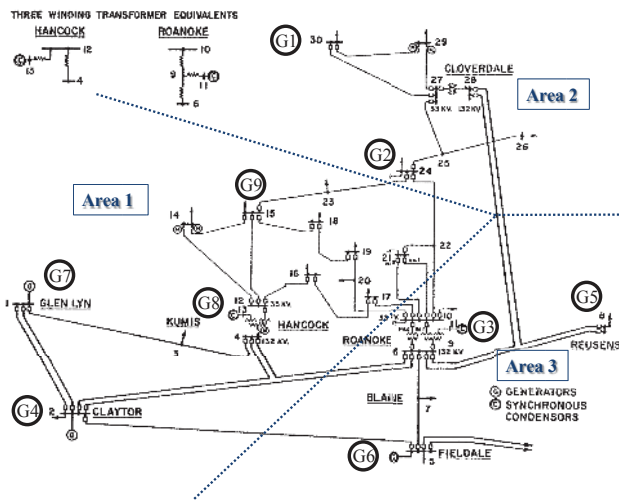
Fig. 12. The topology of IEEE 30-bus test system [34].

$55,135.74 per hour in the 30-bus test system. Similar to the results of the 3-bus test system, the average LMP and the social welfare increase to 40.6 dollar/MWh and $63,464.73 per hour, respectively, estimated by the proposed analytical model at the 60% of the EV penetration level. This is because more transmission congestions appear (e.g., line $(15, 18)$) and more expensive generators (e.g., $G3$ and $G4$) are thus required to serve the load increment. It can be concluded that the EV wireless charging indeed affects the LMP.

The LSE pricing mechanism is investigated to further improve the social welfare of the electricity market. First, we assume that all the LSEs in different areas assign the same retail price on each bus. The average LMP of area 1, area 2, and area 3 dramatically drop from 39.6 to 24.33, from 38.26 to 24.28, and from 42.05 to 23.76, respectively, when the retail price raises from 4.5 to 6.5 cent/kWh. This is because more EV owners do not charge their batteries under the higher retail price. Thus, the transmission congestion of line $(15, 18)$ is relieved and the power output of generator $G3$ and $G4$ is largely reduced. However, the social welfare does not increase as a result of the increment of the retail price. Reducing the wireless charging load may decrease the LSE revenue more significantly than the reduction in the GENCO generation cost. When the retail prices of all the areas are set as 5.5 cent/kWh, the highest social welfare ($65,827.89 per hour) is achieved. Then, we consider all combinations of the retail price from 4.5 to 6.5 cent/kWh for the three areas. Among all the combinations, the maximum social welfare ($66,028.59 per hour) is obtained by choosing the pricing mechanism with, 5.5 cent/kWh for the area 1, 5.5 cent/kWh for the area 2, 6 cent/kWh for the area 3. It matches the result presented in Subsection IV-E. The social welfare can be enhanced by raising the retail price of the area with the higher LMP (i.e., the area 3 in the case study).

VI. Conclusion and Future Work

In this paper we have proposed a BCMP network model to predict EV wireless charging demand for investigating the impact of EV wireless charging and mobility on the LMP.

Based on the traffic statistics and power system configurations, the proposed model can capture the dynamics of EV mobility and then compute the wireless charging load. The LMP and the social welfare are thus calculated based on economic dispatch. The LSE pricing mechanism is investigated to reduce the LMP variations and maximize the social welfare. The validity of the proposed BCMP network model has been confirmed by computer simulations using the SUMO realistic traffic simulator. The results have shown that the proposed BCMP network model accurately predicts the wireless charging load and the wireless charging load increases the LMP variations of each bus in the power system. Moreover, the proper pricing mechanism not only suppresses volatility of LMP on certain buses but also increases the social welfare. For further research, we intend to carry out more theoretical investigation on related topics (e.g., investigating the impact of EV wireless charging on microgrids [36] and developing techniques for EV optimal battery management [37], [38]). In addition, the design and incorporation of charging stations in the proposed system is another interesting research topic [39]. The experimental or field evaluation of on-road wireless charging system will be conducted when the implementation of wireless charging system becomes mature.

References

[1] J. Gozalvez, "First wireless electric vehicle charging trial," *IEEE Vehicular Technology Magazine*, vol. 7, no. 2, pp. 10–17, June 2012.

[2] Y. J. Jang, Y. D. Ko, and S. Jeong, "Optimal design of the wireless charging electric vehicle," in *Proceedings of IEEE International Electric Vehicle Conference (IEVC)*, pp. 1–5, Mar. 2012.

[3] X. Yu, S. Sandhu, S. Beiker, R. Sassoon, and S. Fan, "Wireless energy transfer with the presence of metallic planes," *Applied Physics Letters*, vol. 99, no. 21, pp. 214102–214102-3, Nov. 2011.

[4] S. Chopra and P. Bauer, "Driving range extension of EV with on-road contactless power transfer - a case study," *IEEE Transactions on Industrial Electronics*, vol. 60, no. 1, pp. 329–338, Jan. 2013.

[5] U. K. Madawala and D. J. Thrimawithana, "A bidirectional inductive power interface for electric vehicles in V2G systems," *IEEE Transactions on Industrial Electronics*, vol. 58, no. 10, pp. 4789–4796, Oct. 2011.

[6] S. Han, S. Han, and K. Sezaki, "Development of an optimal vehicle-to-grid aggregator for frequency regulation," *IEEE Transactions on Smart Grid*, vol. 1, no. 1, pp. 65–72, June 2010.

[7] E. Sortomme and M. A. El-Sharkawi, "Optimal charging strategies for unidirectional vehicle-to-grid," *IEEE Transactions on Smart Grid*, vol. 2, no. 1, pp. 131–138, Mar. 2011.

[8] S. Shao, M. Pipattanasomporn, and S. Rahman, "Demand response as a load shaping tool in an intelligent grid with electric vehicles," *IEEE Transactions on Smart Grid*, vol. 2, no. 4, pp. 624–631, Dec. 2011.

[9] S. Shao, M. Pipattanasomporn, and S. Rahman, "Grid integration of electric vehicles and demand response with customer choice," *IEEE Transactions on Smart Grid*, vol. 3, no. 1, pp. 543–550, Mar. 2012.

[10] K. Qian, C. Zhou, M. Allan, and Y. Yuan, "Modeling of load demand due to EV battery charging in distribution systems," *IEEE Transactions on Power Systems*, vol. 26, no. 2, pp. 802–810, May 2011.